Optical determination of the electron effective mass of strain compensated $In_{0.4}Ga_{0.6}As_{0.995}N_{0.005}$/GaAs single quantum well

LiFang Xu,[a] D. Patel, and C. S. Menoni
Department of Electrical and Computer Engineering, Colorado State University, Fort Collins, Colorado 80523-1373

J. Y. Yeh and L. J. Mawst
Reed Center for Photonics, Department of Electrical and Computer Engineering, University of Wisconsin-Madison, Madison, Wisconsin 53706

Nelson Tansu
Center for Optical Technologies, Department of Electrical and Computer Engineering, Lehigh University, Bethlehem, Pennsylvania 18015

(Received 6 August 2006; accepted 31 August 2006; published online 24 October 2006)

A detailed line shape analysis of the temperature dependent *photoluminescence* spectra of $In_{0.4}Ga_{0.6}As_{1-y}N_y$/GaAs quantum well (QW) ($y=0,0.005$) is carried out and the relative contribution of free excitons and free carriers to the radiative recombination at different temperature is quantitatively assessed. The analysis extracts the binding energy of the e_1-hh_1 ground-state exciton which equals 9.72 ± 1.24 and 17.5 ± 0.9 meV for InGaAs and InGaAsN (N=0.5%) single QW sample, respectively. By using a fractional dimension exciton binding energy model, an electron effective mass of $m_e^*=(0.11\pm0.015)m_0$ is determined for the highly strained dilute nitride single QW. © *2006 American Institute of Physics*. [DOI: 10.1063/1.2364068]

The growth of high indium content InGaAsN quantum wells (QWs) of high quality on a GaAs platform has been key to realize the best performance of 1.3 μm laser diodes based on this material system.[1–3] Despite these recent laser successes, many fundamental physical parameters of the high indium content InGaAsN are virtually unknown. For instance, to date no direct determination of the electron effective mass m_e^*, has been reported for high indium content (~30%–40%) $In_xGa_{1-x}As_yN_{1-y}$, due to the limitations imposed by the high strain in growing thick freestanding epilayers (typically ~1–3 μm) or QWs with different thickness.

There are model calculations and a few experiments that have investigated the effect of nitrogen on the electron effective mass m_e^*. From the modeling standpoint there are basically two approaches to predict m_e^*, the phenomenological relationship[4] and the band anticrossing model.[5,6] However, these two approaches yield quite different enhancement of m_e^* with nitrogen. The former predicts $m_e^*=0.069m_0$ while in the latter $m_e^*=0.083m_0$. The experiments, mainly conducted on low In-content alloys, report values of m_e^* ranging from $0.08m_0$ to $0.12m_0$.[7–9] The large spread in the experimental results may arise from the method used to determine m_e^*, which relies on the fitting of the optical transitions and requires knowledge of the band-offset ratio that is still relatively controversial.

In this letter, the conduction band edge electron effective mass m_e^* for $In_{0.4}Ga_{0.6}As_{1-y}N_y$/GaAs single QWs is obtained by using a fractional dimension model[10] to fit the exciton binding energy extracted from the line shape analysis of the photoluminescence (PL) at different temperatures. This method is less sensitive to the band-offset ratio and hence allows a more precise determination of m_e^*. The exciton binding energy in $In_{0.4}Ga_{0.6}As_yN_{1-y}$ increases from 9.72 to 17.5 meV when the nitrogen content y is changed from 0% to 0.5%. This results in a change of the electron effective mass from $(0.049\pm0.007)m_0$ to $(0.11\pm0.015)m_0$.

The strain compensated $In_{0.4}Ga_{0.6}As_{0.995}N_{0.005}$/GaAs QW samples used in the experiment were grown by low pressure (200 mbars) and low temperature (530 °C) metal-organic chemical vapor deposition on a GaAs substrate.[1] This structure consists of a 6 nm $In_{0.4}Ga_{0.6}As_{0.995}N_{0.005}$ single QW sandwiched between a GaAs barrier of 300 nm thick. Partial strain compensation of the highly compressively strained QW is achieved by utilizing two 7.5-nm-thick $GaAs_{0.85}P_{0.15}$ tensile strain layers offset 10 nm from the QW and a tensile strain buffer layer of $GaAs_{0.67}P_{0.33}$. A more well understood and widely studied nitrogen-free InGaAs/GaAs QW, with exactly the same structure as the dilute nitride sample, is also investigated as a reference to validate the fitting results for the exciton binding energy and electron effective mass.

For the PL measurement, the samples were mounted on a cold finger of a closed-cycle helium cryostat that allows varying the temperature from 10 to 300 K. PL was excited by a mode-locked Ti:sapphire laser emitting 800 nm pulses with 100 fs duration and 82 MHz repetition rate. Typical average excitation intensity *absorbed* by the sample was 0.5 W/cm^2. Assuming that each 1.55 eV photon generates one electron-hole pair, the corresponding photoexcited sheet carrier density equals 2×10^{10} cm^2. The PL was analyzed by a 2/3 m single grating spectrometer with a spectral resolution of 0.2 nm and detected by a nitrogen cooled InGaAs detector using lock-in technique.

The temperature dependent PL spectra for InGaAsN and InGaAs QWs are shown in Fig. 1. Relevant features of the PL spectra are the following: (1) the broader linewidth of InGaAsN PL compared to InGaAs and (2) the distinct change from Gaussian-like to asymmetric line shape induced by the temperature increase in both samples. The latter sug-

[a]Electronic mail: lfxu@engr.colostate.edu

0003-6951/2006/89(17)/171112/3/$23.00 © 2006 American Institute of Physics

Downloaded 20 Jul 2011 to 128.180.137.141. Redistribution subject to AIP license or copyright; see http://apl.aip.org/about/rights_and_permissions

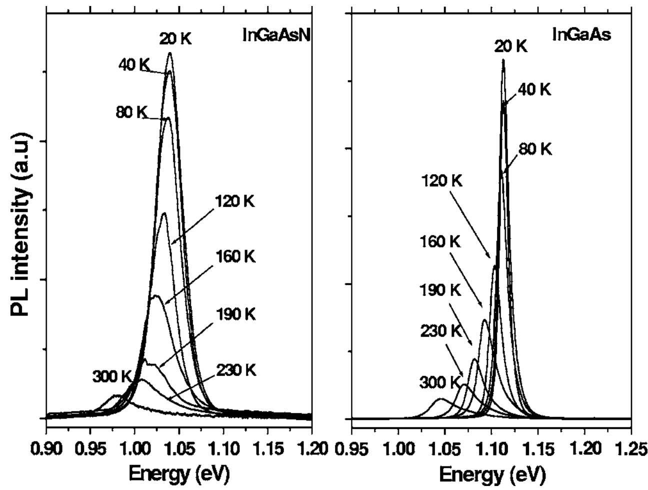

FIG. 1. PL spectra of InGaAs (right) and InGaAsN (left) at various temperatures under an excitation power of 0.25 mW.

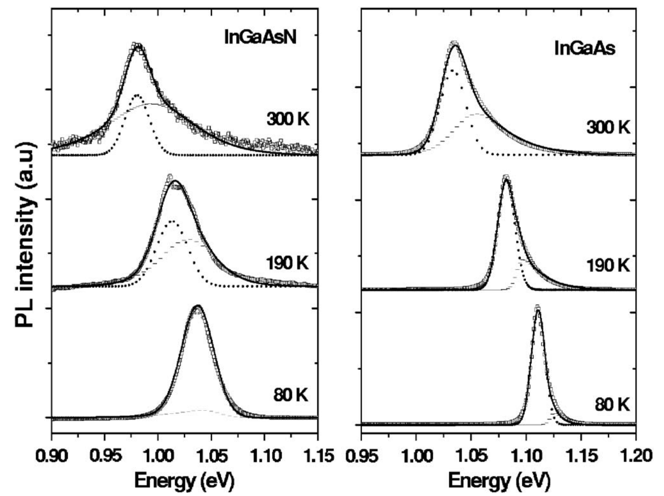

FIG. 2. Fit (solid line) of the PL spectra line shape normalized to the peak (open circle) at different temperatures for InGaAs (right) and InGaAsN (left). The contributions from exciton recombination (dotted line) and free carrier recombination (dashed line) are shown in the graph.

gests an increased contribution from free carrier recombination as temperature increases.

The data of Fig. 1 were analyzed using a simple statistical model proposed in Ref. 11. In this model the PL spectrum is assumed to be a superposition of excitonic and free carrier recombinations. The exciton line can be reasonably taken into account by means of a Gaussian profile multiplied by the Fermi-Dirac statistical distribution function, as shown in Eq. (1). The free carrier recombination term is modeled by an analytical expression that contains the contribution from high-k states. As shown in Eq. (2), this expression incorporates a broadened steplike two-dimensional density of states multiplied by the Fermi-Dirac distribution of the free electrons and holes, and a two-dimensional Sommerfield factor that accounts for the Coulomb interaction between carriers. Thus, the PL emission intensity is the sum of Eqs. (1) and (2),

$$I_x(E) = A_x \exp\left(-\frac{(E-E_H(T))^2}{2\sigma_H^2(T)}\right) \times \frac{1}{1+\exp([E-E_H(T)]/k_BT)}, \tag{1}$$

$$I_C(E) = A_C \frac{1}{1+\exp(-[E-E_C(T)]/\sigma_C(T))} \times \frac{2}{1+\exp(-2\pi\sqrt{R/|E-E_C(T)|}} \times \frac{1}{1+\exp([E-E_C(T)]/k_BT)}, \tag{2}$$

where $A_x(A_C)$, $E_H(E_C)$, and $\sigma_H(\sigma_C)$ are the amplitude, peak energy, and broadening fitting parameters of the e_1-hh_1 exciton (free carrier) recombination, respectively. R is the binding energy of the exciton that needs to be determined, with $E_C = E_H + R$.

The fit of the PL spectra of InGaAs and InGaAsN single QWs with sum of Eqs. (1) and (2), shown in Fig. 2, describes satisfactorily the main features of the PL peaks. It can be seen that as temperature rises, the relative contribution of the exciton emission decreases, while the free carrier's contribution increases.

The integrated exciton and free carrier area emissions obtained from the fit were assumed to be proportional to the free exciton (N_x) and free carrier (N_e, N_h) populations, respectively. This is the case, as the recombination coefficient for both excitons and free carriers has the same temperature behavior.[12] Figure 3 depicts the semilogarithmic variation of the ratio of free carriers to exciton populations, $(N_eN_h/N_x) \times (1/T)$, as function of $1/k_BT$, which is linear for both InGaAs and InGaAsN. Plotted in this format, the data of Fig. 3 can be fitted with the two-dimensional law of mass action,[13]

$$\rho = \frac{N_eN_h}{N_x} \propto \frac{m_em}{m_e+m_h}\frac{k_BT}{\pi\hbar^2}e^{-(R/k_BT)}, \tag{3}$$

to obtain from the slope of Fig. 3 the exciton binding energy R. Since the exciton binding energy is also a parameter used in the line shape fitting of the PL spectra, a careful iteration was implemented to extract R that fits simultaneously the data of Figs. 2 and 3. Based on this fitting procedure, the

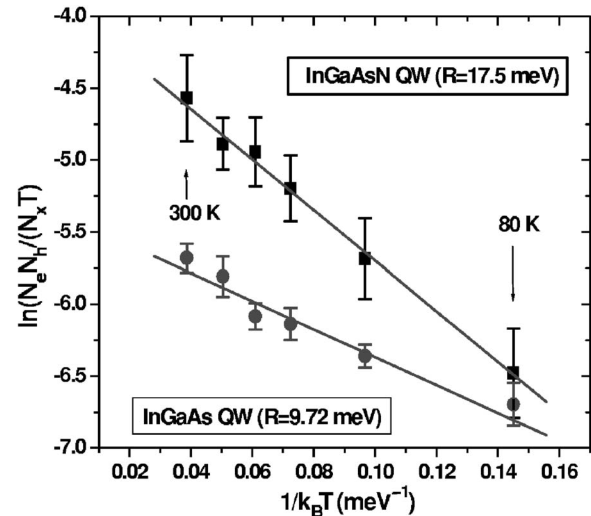

FIG. 3. Semilogarithmic plot of $N_eN_h/(N_xT)$ as function of $1/k_BT$ from both InGaAs and InGaAsN QW (symbols). The straight lines are the best fit to the experimental data using the 2D mass law. The slope yields the exciton binding energy R indicated on the figure.

Downloaded 20 Jul 2011 to 128.180.137.141. Redistribution subject to AIP license or copyright; see http://apl.aip.org/about/rights_and_permissions

TABLE I. Parameters for the calculation of electron effective mass at band edge.

Material	Heavy hole mass m_{hh}^*	Well depth conduction band (meV)	Well depth valence band (meV)	Luttinger parameter γ_1	Dielectric constant ε
$In_{0.4}Ga_{0.6}As$	$0.457m_0$	306	165	12.188	13.9
$In_{0.4}Ga_{0.6}As_{0.995}N_{0.005}$	$0.457m_0$	451	99	12.188	13.9
GaAs barrier	$0.51m_0$			6.98	12.9

e_1-hh_1 exciton binding energy was determined to be 9.72 ± 1.24 and 17.5 ± 0.9 meV for InGaAs QW and InGaAsN QW, respectively.

The analysis just described was combined with a simple theoretical calculation based on a fractional dimension model proposed in Ref. 10 to obtain the electron effective mass m_e^*. Within this framework, the ground-state e_1-hh_1 exciton binding energy is given by

$$R=\left(\frac{2}{\alpha-1}\right)^2 R_y, \quad (4)$$

where $R_y=(\varepsilon_0/\varepsilon)^2(\mu/m_0)R_H$ is the exciton Rydberg energy, expressed in terms of m_0, the free electron mass, μ the exciton reduced mass $1/\mu=1/m_e^*+1/m_h^*$, and $R_h=13.6$ eV. Here the parameter α is a fractional dimension value, which varies between 2 and 3 in a real quantum-well structure. The values $\alpha=3$ and $\alpha=2$ give $R=R_y$ and $R=4R_y$, respectively, corresponding to the well-known results for bulk and two-dimensional (2D) infinite quantum-well cases. Thus solving for the exciton binding energy from Eq. (4) consists of defining the spatial dimension parameter α, which is expressed as

$$\alpha=3-e^{-\overline{L_w}/2\overline{a_0}}. \quad (5)$$

Here $\overline{L_w}$ is the effective QW width, representing the spatial extension of the electron and hole wave function which can be obtained by solving Schrödinger's equation. $\overline{a_0}$ is the effective Bohr radius, $\overline{a_0}=(\varepsilon/\varepsilon_0)(m_0/\bar{\mu})a_H$, where $\bar{\mu}$ is the mean value of the three-dimensional reduced mass of the exciton, which is given by $1/\bar{\mu}=1/\overline{m_e^*}+\overline{\gamma_1}/m_0$. $\bar{\gamma}_1$ is the mean value of the Luttinger parameter and $\overline{m_e^*}$ is the mean value of electron effective mass. All mean values of the parameters used here are positionally weighted across the GaAs heterostructure.

Using Eqs. (4) and (5) we calculated m_e^* from the measured exciton binding energy R on the well-studied InGaAs/GaAs QW first. Using the parameters summarized in Table. I,[14] the analysis yielded a fractional dimension parameter $\alpha=2.248$ and a band edge electron effective mass $m_e^*=(0.049\pm0.007)m_0$, which is in good agreement with the established value of $m_e^*=(0.047m_0)$.[15]

Similar calculations were carried out in InGaAsN using the band-offset ratio given in Ref. 14 and the parameters in Table I. The fractional dimension parameter was found to be $\alpha=2.199$. The electron effective mass for InGaAsN was calculated to be $m_e^*=(0.11\pm0.015)m_0$, considering that the dielectric constant and hole effective mass m_h^* do not change sizably upon the incorporation of nitrogen. Notice that the value $\alpha=2.199$ for the InGaAsN single QW is not significantly different from $\alpha=2.248$ obtained for the InGaAs QW, indicating that the band-offset ratio does not strongly influence the calculation of the electron effective mass from exciton binding energy. This larger value of m_e^* is in reasonably good agreement with those reported.[7–9] Unlike these previous experiments which are heavily dependent on the knowledge of the band-offset ratio, our method is proven to be less sensitive on the choice of band-offset ratio, thus providing more reliable results.

In summary, we have performed a detailed PL line shape analysis as function of temperature for strain compensated InGaAsN/GaAs QW that allowed extraction of the relative contribution from excitons and free carriers to the radiative emission. This analysis allowed extraction of the exciton binding energy which was found to increase from $R=9.72$ meV to $R=17.5$ meV when the nitrogen content in the single InGaAsN QW increases from 0% to 0.5%. The electron effective mass was obtained from the exciton binding energy using a fractional parameter model. This approach yielded $m_e^*=(0.049\pm0.007)m_0$ and $m_e^*=(0.11\pm0.015)m_0$ for InGaAs and InGaAsN. The excellent agreement obtained in m_e^* for InGaAs verifies the validity of our approach, which in turn is more accurate as it is less sensitive to variations in the band-offset ratio.

This work is supported by the National Science Foundation under Grant No. ECS 03134410.

[1] N. Tansu, J. Y. Yeh, and L. Mawst, IEEE J. Sel. Top. Quantum Electron. **9**, 1220 (2003).
[2] V. Gambin, W. Ha, M. Wistey, H. Yuen, S. R. Bank, S. M. Kim, and J. S. Harris, IEEE J. Sel. Top. Quantum Electron. **8**, 795 (2002).
[3] J. Y. Yeh, N. Tansu, and L. J. Mawst, Electron. Lett. **40**, 739 (2004).
[4] W. W. Chow, E. D. Jones, N. A. Modine, A. A. Allerman, and S. R. Kurtz, Appl. Phys. Lett. **75**, 2891 (1999).
[5] J. Wu, W. Shan, and W. Walukiewicz, Semicond. Sci. Technol. **17**, 860 (2002).
[6] S. Tomic, E. P. O'Reilly, R. Fehse, S. J. Sweeney, A. R. Adams, A. D. Andreev, S. A. Choulis, T. J. C. Hosea, and H. Riechert, IEEE J. Sel. Top. Quantum Electron. **9**, 1228 (2003).
[7] Z. Pan, L. H. Li, Y. W. Lin, B. Q. Sun, D. S. Jiang, and W. K. Ge, Appl. Phys. Lett. **78**, 2217 (2001).
[8] M. Hetterich, M. D. Dawson, A. Y. Egorov, D. Bernklau, and H. Riechert, Appl. Phys. Lett. **76**, 1030 (2000).
[9] J. B. Heroux, X. Yang, and W. I. Wang, J. Appl. Phys. **92**, 4361 (2002).
[10] H. Mathieu, P. Lefebvre, and P. Christol, Phys. Rev. B **46**, 4092 (1992).
[11] M. Colocci, M. Gurioli, and A. Vinattieri, J. Appl. Phys. **68**, 2809 (1990).
[12] P. K. Basu, *Theory of Optical Processes in Semiconductors: Bulk and Microstructures* (Oxford University Press, New York, 2002), pp. 203–234.
[13] D. S. Chemla, J. Lumin. **30**, 502 (1985).
[14] N. Tansu and L. J. Mawst, J. Appl. Phys. **97**, 054502 (2005).
[15] I. Vurgaftman, J. R. Meyer, and L. R. Ram-Mohan, J. Appl. Phys. **89**, 5815 (2001).

Downloaded 20 Jul 2011 to 128.180.137.141. Redistribution subject to AIP license or copyright; see http://apl.aip.org/about/rights_and_permissions